

Conditional recovery of time-reversal symmetry in many nucleus systems

Yoritaka Iwata^{1*} and Paul Stevenson²

¹*Institute of Innovative Research, Tokyo Institute of Technology, Japan and*

²*Department of Physics, University of Surrey, United Kingdom*

(Dated: September 28, 2018)

Propagation of non-topological soliton in many-nucleus systems is studied based on time-dependent density functional calculations with focusing on mass and energy dependence. The dispersive property and the nonlinearity of the system, which are inherently included in the nuclear density functional, are essential factors to form a non-topological soliton. On the other hand the soliton propagation is prevented by the charge equilibration dynamics, and the competition possibly appears. In this article, based on the energy-dependence of the two competitive factors, the concept of conditional recovery of time-reversal symmetry is proposed in many nucleus systems. It clarifies a possibility of preserving nuclear medium inside natural or artificial nuclear reactors, under a suitable temperature. From an astrophysical point of view, the existence of the low-temperature solitonic core of compact stars is suggested.

PACS numbers: 05.45.Yv, 25.70.Hi, 26.50.+x, 28.90.+i, 21.60.Jz

The dispersion property and nonlinearity are essential to the existence of non-topological solitons, where a non-topological soliton means a wave propagating with perfect transparency. The nonlinear Schrödinger equation (for a textbook, see [1])

$$i\partial_t\psi(x,t) = -\partial_x^2\psi(x,t) - 2g|\psi(x,t)|^2\psi(x,t)$$

is a typical example exhibiting bright solitons for $g > 0$ in which the first and the second terms of the right hand side are responsible for the dispersive property and nonlinearity, respectively.

From a more physical point of view, soliton propagation in quantum systems depends substantially on the collective degree of freedom. In the case of atomic nuclei, the fast charge equilibration [2], which is a kind of quantum and fermionic many-body effect, prevents soliton propagation. Indeed the formation of a uniform charge distribution is led by the charge equilibrating wave, while the independence of a non-uniform density distribution is conserved by the soliton wave. According to a comparison to other nuclear theories and experiments [3–7], an almost universal propagation speed several tens of percent slower than the fermi velocity (corresponding to almost 25% of the speed of light for many nucleon systems) is found for the fast charge equilibration, and it is suggested to be associated with the zero sound propagation [8] of the many-nucleon system [9]. This propagation speed is higher than the relative velocities of low-energy ion collisions. Since the soliton propagation speed is definitely given by the relative velocity of collisions, the soliton wave propagation is expected to be effectively prevented by the fast charge equilibrating wave in low-energy ion collisions. This is an intuitive explanation for the mechanism for the energy-dependent existence of soliton propagation [10] in nuclei, where there is an upper energy

limit for the appearance of the fast charge equilibrating wave [2]. Accordingly, non-topological soliton propagation in many nucleon systems should be different in its typical order of propagation speed compared with other cases such as soliton propagation in many quark systems. In addition the nuclear symmetry energy is expected to play a role in soliton propagation, as it is the main driving force of the fast charge equilibration [11].

In this article a realization of the mathematical concept of non-topological solitons is presented in sub-atomic fermionic systems. Some special conditions must be satisfied for the existence of the soliton in a system of interacting nuclei, because the medium consists of two components: protons and neutrons. In this sense non-topological soliton propagation in many-nucleus systems is found to be essentially different from that in optics (massless single component system) or electron systems (single component system). As a result, the conservation inherent to non-topological soliton leads to the conditional recovery of time-reversal symmetry in many-nucleus systems. Possible application of non-topological soliton is presented from astrophysics to nuclear engineering.

The nuclear medium confined in reactors, stars and so on consists of many kinds of nucleus in which the statistical nuclear kinetic energy determines the temperature of nuclear medium. Meanwhile, the nucleus is a many-nucleon system, which consists of protons and neutrons, and is a nonlinear system interacting by the nuclear and the Coulomb forces. In order to understand the soliton propagation in many nucleus system, it is ideally studied by including detailed nucleon degrees of freedom. For the existence of non-topological soliton propagation, the competition between the nonlinear transparency and the charge equilibration is essential at the level of nucleon degrees of freedom. Those two mechanisms compete with each other; indeed the former one prevents mixing the two species of nucleon while the latter one contributes to form a mixed nuclear medium with a certain neutron-to-

*Electronic address: iwata_phys@08.alumni.u-tokyo.ac.jp

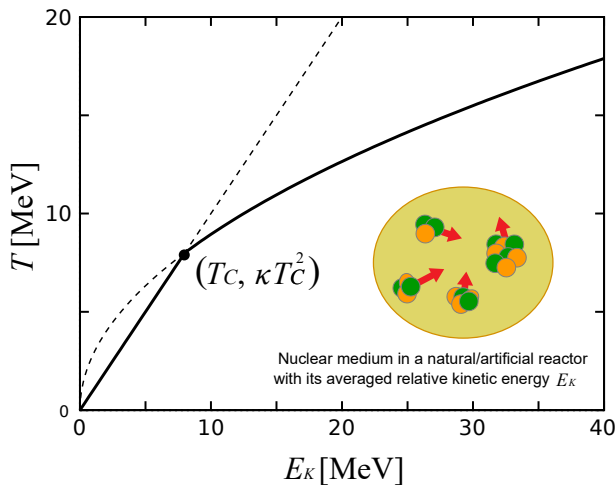


FIG. 1: (Color online) A model for many-nucleus system is shown by a thick line. Temperature is estimated by Eq. (1) with $T_C = 7.2$ MeV. E_K is the relative kinetic energy of a representative nucleus in the many-nucleus system. Note that $(T_C, \kappa T_C^2)$ always satisfies Eq. (1) independent of the choice of T_C and κ . In the present examination soliton propagation is studied for low-energy medium with temperature below 30 MeV. The inserted figure illustrates nuclear medium in our scope, where each nucleus is made of protons and neutrons, and the momentum vectors of nuclei are shown by red arrows.

proton number ratio (N/Z ratio). Temperature control is expected to be possible if the conditions from the two mechanisms allow a meeting energy range.

An order estimation for the temperature of many-nucleus system (not of many-nucleon system) is necessary, and it is provided by following the manner used in many-nucleon system. Employing the definition of temperature of nucleus (many-nucleon system) utilizing the Bethe formula [17, 18], the temperature of many-nucleus system is estimated by

$$E_K = \begin{cases} \kappa T_C T, & T \leq T_C \\ \kappa T^2, & T > T_C \end{cases} \quad (1)$$

where two parameters are included; T_C defines the border between high and low temperatures, and it is reasonable to take $T_C = \kappa^{-1} = 7.2$ MeV [2]. Note that $T_C = 7.2$ MeV is associated with the translation of the fermi energy of many-nucleon system to the relativistic center-of-mass kinetic energy [19]. In low energies, a real constant κ corresponds to a proportional constant between E_K and T_C (cf. the Boltzmann factor). It behaves linearly for low temperature and quadratically for high temperature (Fig. 1). In order to define the temperature, it is necessary to know the relative kinetic energy E_K between nuclei. Here we assume the statistical relative kinetic energy is well approximated by the collision energy of given representative heavy-ion collisions. Since the temperature can be defined in a thermalized statistical ensemble, it is reasonable to assume that the temper-

TABLE I: Self-binding energies of the ground states are calculated using the SV-bas effective interaction. Binding energy per nucleon [MeV/nucleon] of the initial states are compared to those of intermediate states, and the corresponding experimental values are shown in parenthesis [16]. The system for $(A, Z) = (204, 100)$ is too proton-rich to have a bound state.

(A, Z)	$B(^A Z)$	$B(^{A+4} Z)$	$B(^{2A+4} 2Z)$
(4,2)	6.93 (7.08)	4.48 (3.93)	6.07 (7.06)
(16,8)	8.21 (7.98)	7.84 (7.57)	8.75 (8.58)
(40,20)	8.73 (8.55)	8.80 (8.66)	8.59 (8.36)
(48,20)	8.83 (8.67)	8.59 (8.43)	8.60 (8.52)
(100,50)	8.35 (8.25)	8.45 (8.38)	— (—)
(120,50)	8.54 (8.50)	8.51 (8.47)	7.47 (7.47)

ature is unchanged during the heavy-ion collisions, and the temperature is defined by that of initial state. Such a treatment is sufficient to have an order estimation for the temperature of nuclear medium.

Representative ion reactions



in the nuclear medium are considered. In fact reactions of six kinds $(A, Z) = (4, 2), (16, 8), (40, 20), (48, 20), (100, 50)$ and $(120, 50)$ are investigated for clarifying the conservation properties of the nuclear medium. Different N/Z pattern formation of the nuclear medium is expected to appear depending on the combination of Z and N , and the soliton propagation should be altered accordingly. The choice of these combinations follows from a preceding research on nuclear symmetry energy [11] in which the highest achievable density and the corresponding asymmetry parameter δ have been presented for $(A, Z) = (40, 20), (48, 20), (100, 50)$ and $(120, 50)$ cases. Accordingly this examination covers a mass range from 12 to 244. It is notable that reactions of this kind recently collected a special attention in terms of identifying the extraordinary neutron-rich resonance state of the tetra-neutron [12–15]. In the present setting, ^{A+4}Z of several kinds plays a role of mother nuclei for the tetra-neutron.

Central collisions are calculated, since effects of non-central collisions have already been assessed to enhance the soliton property as much as several 10% [10]. That is, central collisions bring about the most strict condition for the realization of the soliton property, and this property is then amenable to the present examination of showing a possible application of the soliton propagation in many-nucleus systems. As a result of these reactions, depending on the collision energy from 1 MeV to several 10 MeV per nucleon, fusion, deep-inelastic collision, and collision-fission such as fusion fission and quasi fission are possible to appear. Table I compares the binding energies of the colliding nuclei to those of intermediate fused systems. For $Z \geq 20$, $B(^{2A+4} 2Z)$ value becomes smaller compared to $B(^A Z)$ and $B(^{A+4} Z)$ values. That is, the

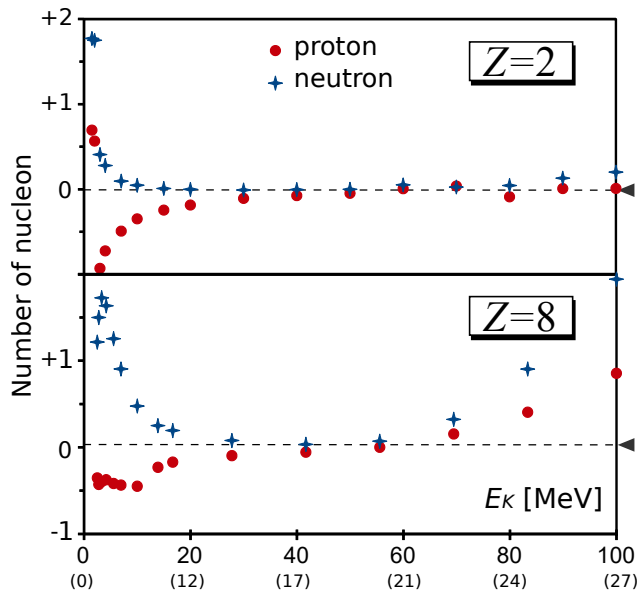


FIG. 2: (Color online) Nucleon transfer took place in reactions (2). Numbers of transferred protons and neutrons from $A+4Z$ to AZ , where $(A, Z) = (4, 2)$ and $(16, 8)$. The horizontal axis shows the energy per nucleon (temperature [MeV] in the parenthesis), and the perpendicular axis shows the number of transferred nucleon. The value becomes positive if nucleon is transferred from $A+4Z$ to AZ , and negative if nucleon is transferred from AZ to $A+4Z$. The fusion events are ignored, so that the lowest energies in graphs correspond to a few MeV. Since the statistical distribution represented by probability wave is calculated in the TDDFT, the calculated nucleon number interpreted as the number probability generally becomes non-integer.

change of reaction type from exothermic to endothermic is the reaction included in the present settings. Incident energies with 1 to 100 MeV per nucleons are taken into account. As in the preceding research [10], the high energy cases around $E_K = 100.0$ MeV are presented for theoretical interest, because the high energy cases with those relative velocity almost equal to 80% of the speed of light lie beyond the application limit of non-relativistic theory employed in the following.

Theoretical investigations are carried out based on the time-dependent nuclear density functional theory (TDDFT, for short). For $r \in \Omega \subset \mathbb{R}^3$ and $t \in \mathbb{R}$, the TDDFT equation is written by

$$i\hbar\partial_t\psi_{q,j}(r,t) = H(\psi_{q,j}(r,t))\psi_{q,j}(r,t), \quad (3)$$

where $\psi_{q,j}(r,t)$ denotes single-nucleon wave function ($j = 1, 2, \dots, 2A + 4$), the index q identifies isospins, and $H(\psi_{q,j}(r,t))$ is the effective Hamiltonian operator used in the nuclear density functional theory (for example, see [20] for the detail representation, and refer to [21] for a mathematically rigorous derivation). Equation (3) is a nonlinear Schrödinger type equation satisfying the dispersive property. At this point the TDDFT is a unique theoretical framework for investigating the soli-

tonic transportation in many-nucleus systems as built upon the nucleon degrees of freedom (for a review of TDDFT including recent developments, see [22]). Due to the Schrödinger type formalism, the TDDFT is the non-relativistic theory whose theoretically-permissible upper limit of the relative kinetic energy is several 10 MeV per nucleon. The spin degree of freedom is also taken into account, although it is not explicitly shown in Eq. (3). Periodic boundary conditions are imposed on both stationary and nonstationary problems. In particular the stationary problem is numerically solved to prepare the initial state consisting of two colliding nuclei with a certain relative velocity. As an effective interaction, the SV-bas nuclear interaction [23] and the Coulomb interaction are implemented. The SV-bas interaction is especially known for well reproducing the neutron skin thickness of heavy nuclei such as ^{208}Pb (for a compilation of experimental and theoretical results, see [24]). This property is expected to be relevant for the stability of the tetra-neutron. Although the pairing interaction is not introduced in the present density functional, the collision energy is sufficient high for pairing interaction not to play a significant role. Indeed, from an energetic point of view, the nuclear pairing is the effect less than a few 100 keV per nucleon. Numerical solutions are obtained based on the finite difference method (for the details, see Ref. [25]). The numerical settings such as time and space unit sizes follow from the preceding research [10]. By comparing to experimental self-binding energies (Table I), the validity of the present theoretical framework can be recognized, where the difference between theoretical and experimental values are less than 4% at the most. The theoretical framework with the numerical settings is concluded to be sufficient to simulate the ion collisions.

Before moving on to the main discussion, we briefly review the preceding results [10]. According to the preceding research dealing with $^4\text{He}+^8\text{He}$ reactions, the dominance of nonlinear t_1 -term $|\psi|^2\psi$ in the density functional has been confirmed. Indeed there cannot be any bound states by switching off the t_1 -term. On the other hand, t_1 -term contribution is highly modified by the secondary-dominant nonlinear fractional power t_3 -term $|\psi|^{2+\alpha}\psi$ (for the dominance, compare the results with and without t_1 and t_3 terms in Table 2 of Ref. [10]). Dominance of those terms in the nuclear density functional implies the validity of an energy-dependent soliton existence in which t_1 -term and t_3 -term are responsible for the soliton existence and energy dependence respectively. It is remarkable here that t_3 -term is known to be indispensable for the reproducing of the incompressibility of nuclear matter and the related excitation states. In Ref. [10], for ion reactions including light ions, the energy-dependence of soliton emergence has been clarified in terms of both mass and momentum transparencies. Rough sketch of the energy-dependence is as follows: the soliton property is not so active for low energies less than a few MeV per nucleon, soliton property becomes active around 10 MeV per nucleon, it achieves almost the perfect transparency

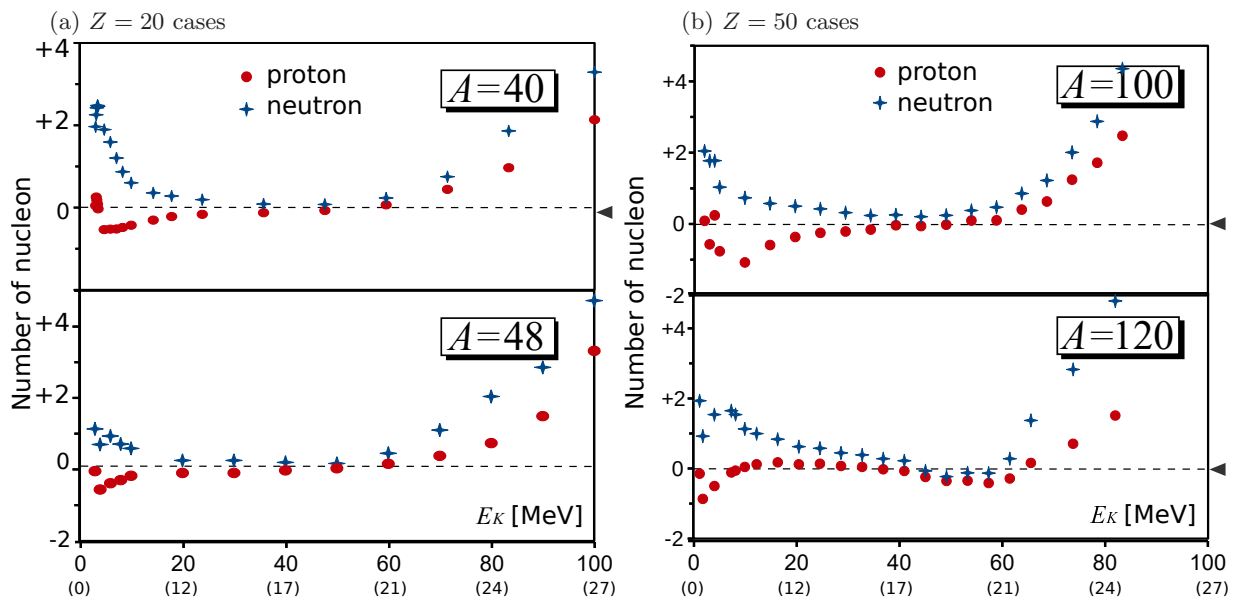


FIG. 3: (Color online) Numbers of transferred protons and neutrons from $A+4Z$ to AZ , where $Z = 20$ is examined in the left, and $Z = 50$ in the right. The drawing manner follows from Fig. 2.

around 20 to 40 MeV per nucleon, and the transparency again decreases for much higher energies.

Figure 2 shows the nucleon transfer for ${}^8\text{He}+{}^4\text{He}$ and ${}^{20}\text{O}+{}^{16}\text{O}$ collisions. First, the similarity between the two cases are noticed. Positive neutron transfer and negative proton transfer appear simultaneously at low temperatures less than 10 MeV. This is classified as a kind of charge equilibration [26], in which proton-rich AZ gains neutrons and loses protons simultaneously. Solitonic transportation events are seen at intermediate temperatures from 10 to 20 MeV. It means that the tetra-neutron independence is true within a limited energy range. As prominently seen in case of $Z = 8$, massive neutron-proton transfers appear for high temperatures above 21 MeV. Indeed AZ gains protons with almost the twice numbers of neutrons (transfer with $N/Z \sim 2$). Not only the charge difference but also the mass difference of the two nuclei becomes smaller in this kind of neutron-proton massive transfer reactions. Since significant numbers of nucleons are emitted from the final products during or promptly after the collision (cf. multi fragmentation) in high temperatures larger than 20 MeV, these reactions undergo momentum equilibration rather than the mass equilibration. More precisely, the transportation at higher energies is understood as the mixture of neutron and deuteron emissions carrying away large amounts of momentum. This is to say, the main stabilization or cooling mechanism of higher energy ion-collisions is confirmed to be nucleon emissions. Second, for the mass dependence, the soliton property is more suppressed in the heavier case. This tendency is not seen in the low temperature side, but prominently in the high temperature side. The prevention of soliton propagation at lower temperature shows the universal validity of fast charge

equilibration mechanism, while the considerable prevention at higher temperature is due to the momentum equilibration mechanism.

The left panels of Fig. 3 compare the nucleon transfer between ${}^{44}\text{Ca}+{}^{40}\text{Ca}$ and ${}^{52}\text{Ca}+{}^{48}\text{Ca}$, and the right panels compare the nucleon transfer between ${}^{104}\text{Sn}+{}^{100}\text{Sn}$ and ${}^{124}\text{Sn}+{}^{120}\text{Sn}$. Solitonic transportation events are seen at intermediate temperatures about 20 MeV. For ${}^{44}\text{Ca}+{}^{40}\text{Ca}$ and ${}^{52}\text{Ca}+{}^{48}\text{Ca}$ reactions, there is no significant difference except for the amount of massive neutron-proton transfers at higher temperatures. Note that momentum equilibration is affected by stable bound states; ${}^{40}\text{Ca}$ is the most stable among $Z = 20$ nuclei, and ${}^{116}\text{Sn}$ is the most stable among $Z = 50$ nuclei. On the other hand, in case of $(A, Z) = (48, 20)$, $(100, 50)$, and $(120, 50)$ reactions, ${}^{50}\text{Ca}$, ${}^{102}\text{Sn}$, ${}^{122}\text{Sn}$ are the charge equilibrated nuclei, respectively. Despite the fact that there is a remarkable difference between the most stable and the charge equilibrated nuclei for a given Z , charge equilibration always appears in lower energy side. Among several features, neutron richness plays a quite limited role in altering the confirmed energy-dependent prevention of soliton propagation. We have confirmed a universal trend that the soliton property is more suppressed in the heavier case.

The soliton independence is broken by the nuclear symmetry energy effect. As seen in Figs. 2 and 3, the breaking mechanism of soliton in lower and higher energy sides are different. Since nuclear symmetry energy is dependent on both its density and temperature, the transportation in extremely high density situations can be different. Although quite a few things are known for nuclear medium at extreme situations at this point, achievable high densities and the corresponding nuclear

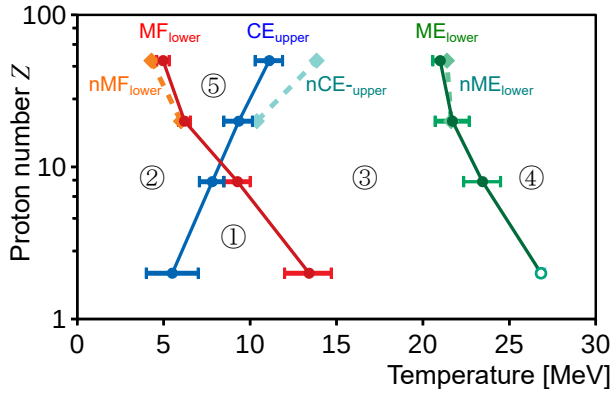


FIG. 4: (Color online) Classification of reaction types depending on the temperature and mass. Charge equilibration upper-limit energy (CE_{upper}) is compared to the multi-fragmentation lower-limit energy (MF_{lower}) and massive momentum transfer lower-limit energy (ME_{lower}). For $N/Z=1$ cases, the error bars are added by the calculated collision energies, the central points of lower side and upper side of error bars are connected by thick lines, where ME_{lower} with $Z = 2$ is calculated to be larger than $T = 29$ MeV (corresponding to the upper bound of our calculation $E_K = 100$ MeV). For $Z = 20$ and 50 cases, $N/Z=7/5$ cases are plotted with dashed lines and without error bars (for the better comparison without any congestion) that are shown by nCE_{upper} , nMF_{lower} and nME_{lower} respectively. As a result, focusing only on $N/Z=1$ cases, there are five areas labeled from ① to ⑤ separated by the thick lines.

asymmetries in some heavy-ion collisions can be found in Ref. [11]. The curvature of E_x -dependence in Fig. 3 are far from the flat one for $N/Z = 7/5$ cases ($A = 48$ and $A = 120$). Consequently the solitonic transportation can be influenced primarily by the total mass of the colliding system (the size of the colliding nuclei: $A = N + Z$), and secondary by the nuclear symmetry energy effect (the detail composition of colliding nuclei: N/Z).

Figure 4 summarizes all the calculated reactions. The boundary energy between charge equilibration calculated in the lower energy and the solitonic transportation is shown by CE_{upper} . The boundary energy between large momentum transfer calculated in the higher energy and the solitonic transportation is shown by ME_{lower} . The boundary energy indicating whether nucleon emission or multi-fragmentation of more than two fragments appears or not is shown by MF_{lower} . In all the boundaries, the neutron or proton is identified to be transferred, if the calculated transferred nucleon number is more than or equal to 0.5. The existence of optimal temperature control for preserving a nuclear medium is seen as area ①. Tetra-neutron is calculated to survive only in these cases, where the momentum of the two colliding nuclei is also well conserved with several % accuracy. Areas ② and ⑤ are classified to the fast charge equilibration. The two nuclei are not easily mixed up in terms of N/Z ratio (charge distribution) in a large area ③ in which localized charge distribution tends to survive. The multi fragmentation

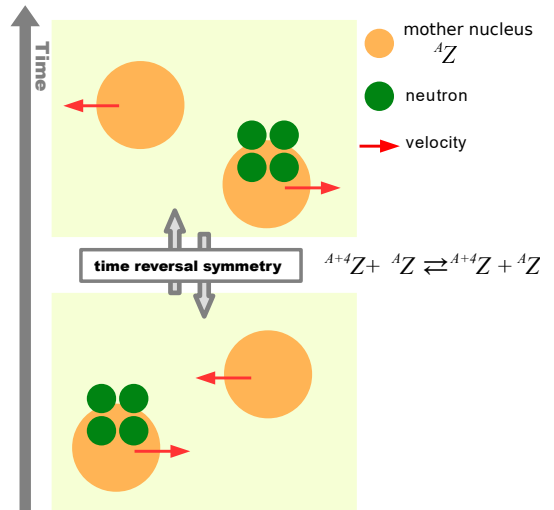


FIG. 5: (Color online) A conservation during ion collisions in which the initial and final nuclei are the same in terms of inclusive neutron and proton numbers, and of the amplitudes of relative momentum of nucleus. Tetra-neutron can be broken depending on the mother nucleus and the momentum.

into small fragments are calculated in an area ④, and therefore the charge distribution tends to be unlocalized. Comparing $N/Z=1$ cases (thick lines) to $N/Z=7/5$ cases (dashed lines), the neutron-richness and thus the nuclear symmetry energy effects play a role to a certain degree. Eventually we conclude that soliton existence and therefore the tetra-neutron independence are mass dependent in the sense of inclusive mother nuclei and its existence can be confirmed only for small mass cases ($Z \leq 8$).

What is clarified by the energy and mass dependent soliton preservation being labeled by Z , A and E_K (corresp. to the area ① of Fig. 4) is associated with the time reversal symmetry. The time reversal symmetry arises from the energy conservation (Fig. 5), as indicated by Noether's theorem. It is worth noting that the total energy conservation is valid to the unitary time evolutions described the TDDFT, while the time reversal symmetry is not necessarily true to the collision dynamics described by the TDDFT because of the appearance of internal single particle excitations and the time-odd components of nuclear energy density functional. The present study suggests the conditional recovery of time-reversal symmetry of certain nuclear medium by a set of light ions ($Z \leq 8$, $A \leq 2Z + 4$) with a certain kinetic energy range.

The concept of low-energy solitonic core or solitonic layer of stellar object is proposed based on the conditional nuclear conservation. Some compact stars are mainly composed of α -particle (^4He); Since the core temperature of compact stars can be from 10 MeV to 20 MeV (e.g., core temperature of white dwarf), α -particle is less reactive to capture neutrons or to form another fused system (Fig. 2), and α -particles are rather well preserved. α -particles are not reactive for certain temperature range,

even if sufficient energy for fusion reactions as much as 10 MeV per nucleon is provided. Meanwhile the soliton star is a long-standing concept whose existence is proposed in association with the relativistic gravitational force field [27] (for a textbook of bosonic stars, soliton stars and the related topics, see [28]). The energy of the soliton stars (comparable to the energy of black holes) is much higher than the present low-temperature solitonic core. Since the temperature range of low-energy soliton propagation is limited from 10 to 30 MeV (Figs. 2 and 3) in the present cases, “low-energy” cold soliton star can exist at only in limited situations, but the solitonic core or solitonic layer of the stellar object is likely to be realized instead.

In conclusion solitonic transportation is shown for many-nucleus systems. A competition between the soliton propagation (a kind of nonlinearity) and the charge equilibration (a kind of many-body property) is essential to the realization of solitons under momentum equilibration. Such a competition is shown to be fully parametrized by the temperature. The results are summarized by the itemization. With focusing on the energy-dependent existence of solitonic transportation in low-energy heavy-ion collisions, a systematic TDDFT calculation shows the following statements:

- the conditional recovery of the time-reversal symmetry is suggested to be valid in many nucleus systems, if they are composed of light nuclei ($Z \leq 8$);
- the independent motion of tetra-neutron is shown

to exist only if the temperature is from 10 to 20 MeV per nucleon;

- from a technological point of view, existence and non-existence of temperature control for preserving nuclear medium is shown to be dependent mainly on the mass of components without being much influenced by the neutron-richness of components;
- from an astrophysical point of view, the concept of low-energy solitonic state for the core of compact star is proposed.

In particular tetra-neutron will find it hard to survive in ${}^4\text{He}+{}^8\text{He}$ reaction if the collision energy is less than 80 MeV per nucleon in the laboratory frame. Tetra-neutron search in ${}^4\text{He}+{}^8\text{He}$ will not show us only some findings for neutron-rich medium, but also the breaking mechanism of time reversal symmetry in femto-meter scale quantum systems. Utilizing the nuclear equation of states to be discovered, the control can be generalized to pressure control or volume control.

Numerical computation was carried out at Yukawa Institute Computer Facility of Kyoto University, and a workstation system at Tokyo Institute of Technology. This work was supported by JSPS KAKENHI Grant No. 17K05440, and UK STFC grant no. ST/P005314/1.

-
- [1] M. J. Ablowitz, *Nonlinear Dispersive Waves: Asymptotic Analysis and Solitons*, Cambridge Univ. Press, 2011.
- [2] Y. Iwata, T. Otsuka, J. A. Maruhn and N. Itagaki, *Phys. Rev. Lett.* **104**, 252501 (2010).
- [3] L. Zhu *et al.*, *Phys. Rev. C* **97** 044614 (2018).
- [4] Y. Zhang *et al.* *Phys. Rev. C* **95** 041602(R) (2017).
- [5] L. Zhu, F. Zhang, P. Wen, J. Su, and W. Xie *Phys. Rev. C* **96** 024606 (2017).
- [6] G. A. Souliotis, P. N. Fountas, M. Veselsky, S. Galanopoulos, Z. Köhley, A. McIntosh, S. J. Yennello, and A. Bonasera *Phys. Rev. C* **90**, 064612 (2014).
- [7] AS Umar, C Simenel and W Ye, *Phys. Rev. C* **96** 024625 (2017).
- [8] A. J. Leggett, *Rev. Mod. Phys.*, **47**, 2, 331 (1975).
- [9] Y. Iwata, *J. Mod. Phys.* **3**, 476 (2012).
- [10] Y. Iwata, *Mod. Phys. Lett. A* **30** 16, 1550088 (2015).
- [11] J. R. Stone, P. Danielewicz, Y Iwata, *Phys. Rev. C* **96** 014612 (2017).
- [12] K. Kisamori, *et al.* *Phys. Rev. Lett.* **116** 052501 (2016) .
- [13] S.C. Pieper, *Phys. Rev. Lett.* **90** 252501 (2003).
- [14] F. M. Marques *et al.* *Phys. Rev. C* **65** 044006 (2002).
- [15] E. Hiyama, R. Lazauskas, J. Carbonell, and M. Kamimura, *Phys. Rev. C* **93** 044004 (2016).
- [16] NuDat 2: <https://www.nndc.bnl.gov/nudat2/>
- [17] H. A. Bethe, *Rev. Mod. Phys.* **9** 69 (1937).
- [18] P. Fröbrich and R. Lipperheide, “Theory of Nuclear Reactions”, Oxford University Press, 1996.
- [19] Y. Iwata, *J. Phys. Conf. Ser.* **445** 012017 (2013).
- [20] D. Vautherin, and D. M. Brink *Phys. Rev. C* **5** 626 (1972).
- [21] Y. Iwata and J. A. Maruhn, a chapter “Energy density functional in nuclear physics” in a book *Density Functional Theory: Principles, Applications and Analysis*, Nova Publishers, 2013.
- [22] C. Simenel, and A. S. Umar, *Prog. Part. Nucl. Phys.* in press (2018).
- [23] P. Klüpfel, P.-G. Reinhard, T. J. Bürvenich and J. A. Maruhn, *Phys. Rev. C* **79** 034310 (2009).
- [24] P. von Neumann-Cosel, *J. Phys. Conf. Ser.* **590** 012017 (2015).
- [25] J. A. Maruhn, P.-G. Reinhard, P. D. Stevenson and A. S. Umar, *Comput. Phys. Commun.* **185** 2195 (2014).
- [26] Y. Iwata, T. Otsuka, J. A. Maruhn, and N. Itagaki, *Nucl. Phys. A* **836** 108 (2010).
- [27] T. D. Lee, *Phys. Rev. D* **35**, 3637 (1987).
- [28] S. L. Liebling, C. Palenzuela, *Living Rev. Relativ.* **20** 5 (2017).